BOUNDARY ELEMENT METHOD EXPERIMENTALLY VALIDATED FOR AN AXIAL AIRFOILS CASCADE

Ionel Doru BACIU[1], Mircea BĂRGLĂZAN[2]

Articolul prezintă o comparaţie între metoda CDF şi un model fizic, amândouă cu aplicate în domeniul mecanicii fluidelor. Ca abordare a problemei a necesitat cea de teorie şi cea de încercare experimentala în domeniul maşinilor axiale reversibile. Problema investigată este abordată de curgerea directă şi inversă a fluidului prin o reţea axiala de profile in "S". Paletele maşinilor turbina-pompa, echipate cu astfel de profile, dovedesc o performanţă bună în curgerea directă şi inversă a fluidului .Pentru modelarea teoretică s-a apelat la metoda elementului de frontieră (MEFr), pentru simulare numerică a curgerii, în reţeaua axială de reţele de profile. Testele experimentale si măsurătorile, au fost efectuate pe tunelul aerodinamic.

This article is a comparison between a CFD-method and a physical model, both applied in the domain of fluid mechanics. The investigated problem was about the direct and reverse fluid flow between a "S" shape chamber of airfoils cascade. Such a task is necessary by the design and operation of axial reversible hydraulic machines. The runner blades of pump-turbines equipped with this kind of profiles shoed good performances in direct and reverse flow directions. Boundary Element Method (BEM) was used for a theoretical model and simulation of the fluid stream and his interaction with the aerodynamic profiles cascade.

Keywords: Boundary Element Method (BEM), CFD-method, aerodynamic, profiles, cascade.

1. Introduction

The rivers, which represent a small part of the earth ocean's volume of water (approx. 2.71%), are today used and harnessed in very different fields of human activity. Taking into account the even more need of water – between other fields also in producing energy – it is very important to utilize in rational, complex and with high efficiencies modes the available water of the rivers.

Hydraulic energy storage for an optimum consumption of the hydraulic potential conducted to hydropower plants with reversible hydraulic machines. The axial hydraulic reversible machines fit well for this purpose.

[1] Assistant, Dept. of Hydraulic Machinery, University "Politehnica"of Timisoara, Romania, e-mail: dodo.i.baciu@gmail.com
[2] Professor, Dept. of Hydraulic Machinery, University "Politehnica"of Timisoara, Romania, e-mail: mbarglazan@yahoo.com

These are the main reason for the present research, namely to realize hydrodynamic profiles, components of the reversible runner blades which operates with high efficiencies as a pump and as a turbine (in generator and motor working condition, with direct and reverse flow).

The best geometry locks to have the "S" shape chamber profiles, from hydrodynamic cascades, investigated in this paper.

2. Boundary element method with linear elements

The digital algorithm for approximate solution of Laplace equation, $\Delta u=0$, in a plane (two-dimensional), close and limited domain, $\overline{\Omega}$ with given boundary conditions may be easy solved through the Boundary Element Method (BEM). The fundamental idea on which is based the BEM is the transformation of the Laplace equation into an integral equation on the boundary of domain.

It is consider Ω, a limited domain in the Euclidian plane R^2 and Γ his boundary. So the boundary element method is given by $\overline{\Omega} = \Omega \bigcup \Gamma$.

Also, it is supposed that the boundary Γ, is smooth on same pieces (it may have a finite number of angular points), with other words the tangent at that the boundary Γ is continuous varying (with some steps). Exception are a finite number of points (nodes) $P_1, P_2,..., P_r \in \Gamma$ where the left values of the tangent, is different from the right values of the tangent. A similar behaviour, identical with the tangent, has the normal $\bar{n}$ on the boundary (see fig.1).

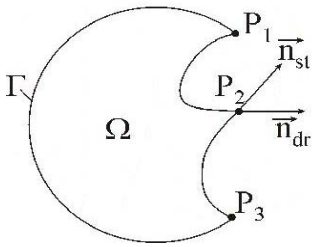

Fig.1 Angular points P_1, P_2, P_3 on the boundary Γ

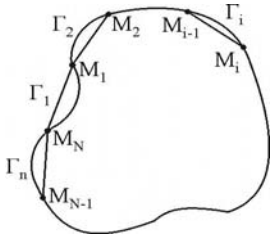

Fig.2 Boundary Γ discretization (meshing)

The Laplace equation is considered on the domain Ω. It may be demonstrated [1], that any solution, *u,* of the Laplace equation checks the integral equation *(1),* which has the form:

$$c(\zeta)\,u(\zeta) = \int_{\Gamma} q(z)\,u^{*}(z,\zeta)\,ds_z - \int_{\Gamma} u(z)\,q^{*}(z,\zeta)\,ds_z, \quad where\ \zeta \in \overline{\Omega} \qquad (1)$$

The function $c(\zeta)$ takes the following values:

$$c(\zeta)=\begin{cases} 1- \quad if\ \zeta\in\Omega,\ \zeta\ is\ inside\ \Omega; \\ \alpha/2\pi - if\ \zeta\in\Gamma,\ where\ \alpha\ is\ the\ angle\ between\ two\ tangent\ in\ a\ corner\ nod; \\ 1/2 - if\ \zeta\in\Gamma\ and\ the\ left\ tangent\ is\ equal\ with\ the\ right\ tangent,\ in\ the\ point\ \zeta. \end{cases}$$

The Laplace equation and the integral equation *(1)* have infinite solutions, so to determine a certain solution it is necessary to impose conditions on the boundary Γ for the function u, respectively for its derivate, $\partial u / \partial n$.

BEM application – with linear elements – imposes two types of approximations:

1) Boundary meshing, see fig.2;
2) Linear approximation of functions u and $q = \partial u / \partial n$, on each element $\Gamma_{i\ of}$ the discretized boundary.

After calculations, equation (1) reduces to a linear system of equations *(2)*:

$$\sum_{j=1}^{N} G_{ij}\, q_j \; - \sum_{j=1}^{N} H_{ij}\, u_j \;=\; 0 \qquad (2)$$

In this system, the unknowns are u_1, u_2, u_N and their derivates $q_1, q_2 \ldots q_N$. The coefficients G_{ij} and H_{ij} are curvilinear integrals (on the segments Γ_j), from known functions.

If $i \neq j$, the integrals which give the values of G_{ij} and H_{ij} don't have singularities and they may be calculated (eq. through the method of numerical quadrature, gauss method).

If $i = j$, the integrals are improper and can be calculated so:

- G_{ii} – are directly calculated and it is obtained:

$$G_{ii} = \frac{l_i}{2}\left[\frac{3}{2} - \ln(l_i)\right] + \frac{l_{i+1}}{2}\left[\frac{3}{2} - \ln(l_{i+1})\right],\quad i = \overline{1,N} \qquad (3)$$

where l_i is the segment Γ_i length ($l_{N+1} = l_1$);

- H_{ii} – are indirectly computed, with the observation that the function $u(z) \equiv 1$ for $z \in \overline{\Omega}$, verifies Laplace equation $\Delta u = 0$; if is applied the above mentioned reason to this function, it are obtained from the relation *(2)*:

$$\sum_{j=1}^{N} H_{ij} \;= 0, \quad i = \overline{1,N} \quad or \quad H_{ii} = -\sum_{i=1, j\neq i}^{N} H_{ij} \qquad (4)$$

So, the integral equation *(1)*, defined on the contour Γ, is reduced to a system of N equations with $2N$ unknowns: the approximate values of the unknown functions u, and the normal derivates in the points $M_1, M_2, \ldots, M_N$.

To establish a certain solution, which corresponds to a concrete problem, in the relations *(2)*, there are generally imposed the values of K parameters u_i and *(N – K)* parameters q_j.

3. Applications of the BEM on axial aerodynamic cascades

The application of BEM with linear elements, for establishing the two-dimensional fluid motion, between the axial aerodynamic cascade of profiles with ”S” shape camber for a nonviscous fluid, was realized through the computer programs, for solving the Laplace equation. With the help of this soft, it is possible to determinate analytic:

- the camber of ”S” profiles from NACA type profile;
- the outline of ”S” profiles from NACA type profile;
- the velocity field on boundary of the cascade airfoils with ”S” shape camber;
- the pressure field through pressure coefficients, defined by $c_p = 1 - \left(\frac{V_{pr}}{V_{am}}\right)^2 = \frac{p_{pr} - p_{am}}{0.5\ \rho_{aer}\ v_{am}^2}$, on the boundary of the airfoils cascade of ”S” shape camber;
- the extension of the analyzed domain;
- the aerodynamic field of the airfoils cascade with ”S” shape camber;
- the velocity field of the aerodynamic cascade with ”S” shape camber of the constitutive profiles and
- the pressure field through pressure coefficients of the aerodynamic cascade with ”S” shape camber of the constitutive profiles.

These programs (soft) may be applied to any axial aerodynamic cascade.

In fig.3 it is given the extension of the analyzed domain for a reversible axial cascade, for a reversible axial cascade of ”S” airfoils.

The hydrodynamic field is represented in fig.4, for the fluid flow in turbine working condition of the reversible axial cascade of ”S” profiles.

The computed results are given in figures 5.

In fig.5a are the values of velocity distribution on the boundary of a ”S” airfoils from the investigated cascade in ”S”.

In fig.5b there are visualized the distribution of pressure coefficient on the boundary of a ”S” airfoils from the investigated cascade in ”S”.

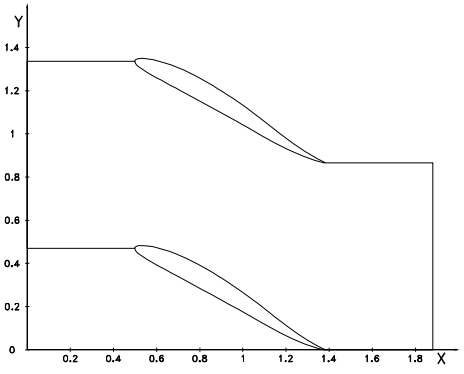

Fig.3 Analysis domain for an axial cascade of "S" airfoils

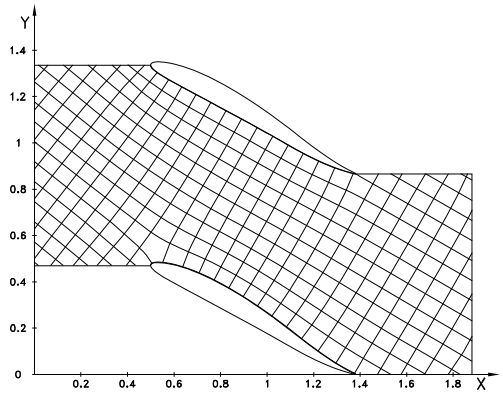

Fig.4 Hydrodynamic field of an axial cascade of reversible airfoils in "S", in turbine working condition

The figures 5a and 5b were calculated for the cascade operation in turbine (motor) working condition.

The investigated cascade has the following parameters: profile chord length $l = 2.2496\ m$, stagger angle $\beta_s = 28.28^0$, pitch to chord ratio $t/l = 0.8663$ with $a = b = t/2l = 0.43321$ and the flow velocity entrance angle $\beta^{AM} = 38.86^0$.

After calculations, it is obtained the values for the parameters: exit angle of the air velocity $\beta^{AV} = 30.12^0$ and the circulation $\Gamma^t = 0.193$ m^2/s.

In fig.6a are the values of velocity distribution on the boundary of a "S" airfoils from the investigated cascade in "S".

In fig.6b there are visualized the distribution of pressure coefficient on the boundary of a "S" airfoils from the investigated cascade in "S".

The figures 6a and 6b were calculated for the cascade operation in generator (pump) working condition. The investigated cascade has the following parameters: geometric are the same like in turbine working condition and the flow velocity entrance angle $\beta^{AV} = 38.86^0$.

After calculations, it is obtained the values for the parameters: exit angle of the air velocity $\beta^{AM} = 30.51^0$ and the circulation $\Gamma^p = 0.0264$ m^2/s.

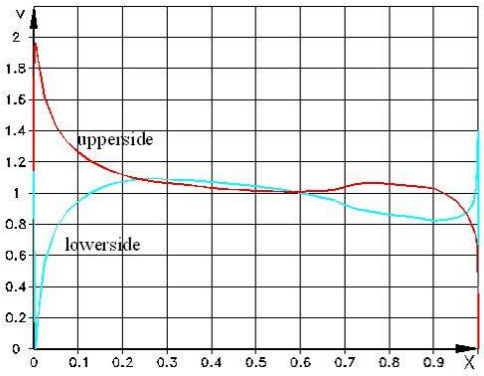

Fig.5a Velocity distribution of the flow on the ”S” shape reversible airfoils boundary in turbine working condition

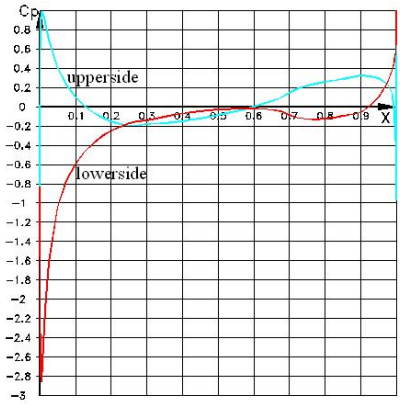

Fig.5b Pressure coefficient distribution on the ”S” shape reversible airfoils boundary in turbine working condition

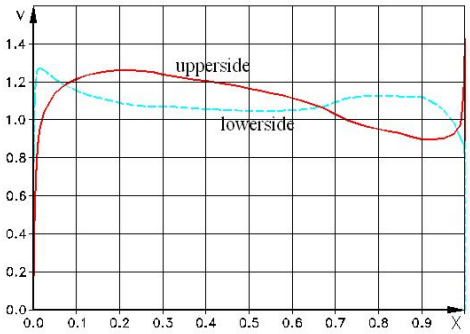

Fig.6a Velocity distribution of the flow on the ”S” shape reversible airfoils boundary in pump working condition

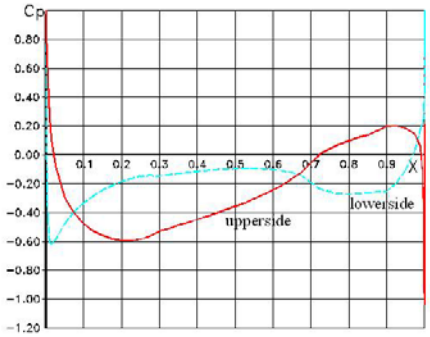

Fig.6d Pressure coefficient distribution on the ”S” shape reversible airfoils boundary in pump working condition

4. Numeric – experimental comparison

The validation of the BEM procedure was made in the aerodynamic tunnel TSLT-40 located in the Hydraulic Machinery Laboratory of the ”Politehnica” University of Timisoara.

The testing rig with the characteristic features is presented in fig.7, a picture of aerodynamic tunnel TSLT-40. In fig.8 are detached some details of rig’s working zone and the measurement apparatuses used by the testing of axial cascade of blades generated from ”S” shape camber airfoils type DIB-024S in pumping and turbine working condition.

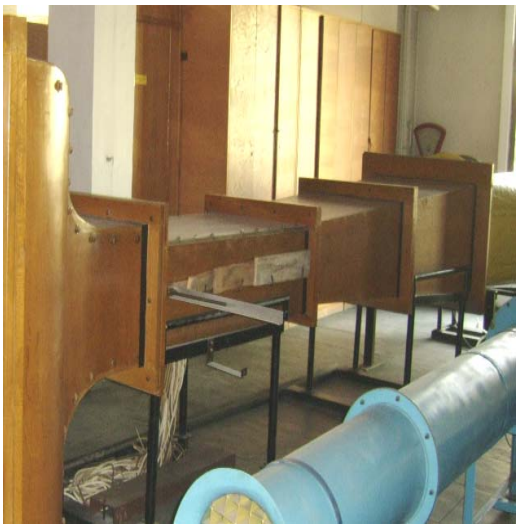

Fig.7b A picture of the TSLT-40 - General set-up.

Fig.8 Testing zone with the chamber for the axial cascade blades generated from "S" airfoils type DIB-024S and the measuring apparatuses

The experimental investigations were made on a middle blade from the airfoils cascade. The "S" shape camber profile was deduced from a NACA 23023 profile and named DIB-024S. The profile chord is 260 mm.

The pressure measurements were made around the contour of the middle profile of the airfoils cascade blades.

The DIB-024S cascade blades had the following pitches: 140, 160, 180 and 200 mm and for each pitch there was considered for stream velocities.

The measured data was processed and finally in the two-dimensional "Cartesian System" of coordinates, stagger angle, β_s and pitch to chord ratio t/l, there was represented the curves of constant maximum values of the pressure coefficients.

For operation in turbine working condition, the above mentioned curves were sketched in fig.9, for the upper side and in fig.10, for the lower side of cascade profile.

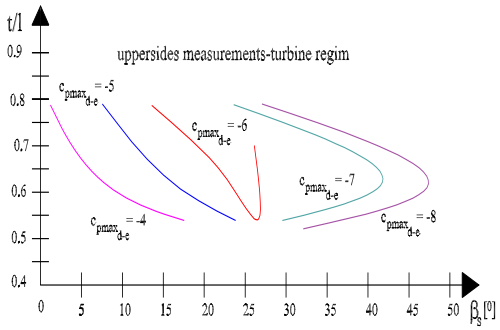

Fig.9 Equal maximum experimentally measured pressure coefficients $c_{p\max}$ = const., on the upper side of the profile DIB-024S from the axial airfoil cascade operating in turbine working condition

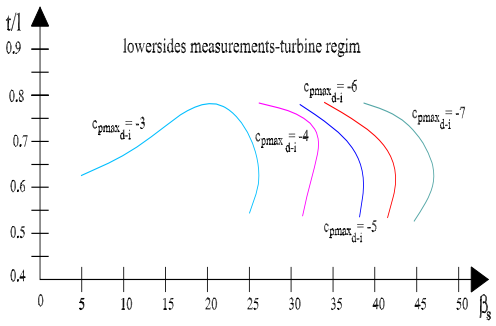

Fig.10 Equal maximum experimentally measured pressure coefficients $c_{p\max}$ = const., on the lower side of the profile DIB-024S from the axial airfoil cascade operating in turbine working condition

For comparison of the experimental results with the theoretical-numerical one, there was modelled and simulated through BEM the same situation. For turbine operation regimes the theoretical results are presented for pressure in fig.11 on upper side and fig.12 on lower side of the axial cascade profiles in "S" operating in turbine regime.

For validation of the theoretical results obtained by CDF soft through BEM with the experimental results, obtained from the tests and the axial cascade of blade, generated from airfoils type DIB-024S, was realized by superposition on the above mentioned results.

For turbine operation regimes these graphics results, for equal maximum pressure coefficient in function of stagger angle β_s and pith to chord ratio t/l, are presented for upper side in fig.13 and for lower side in fig.14, of the DIB-024S type profile from the axial airfoils cascade, in turbine regime.

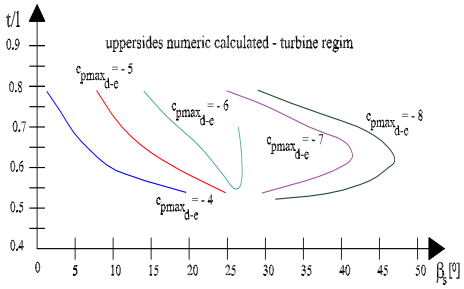

Fig.11 Equal maximum numerical calculated pressure coefficients $c_{p\max}$ = const., on the upper side of the profile DIB-024S from the axial airfoil cascade operating in turbine regime

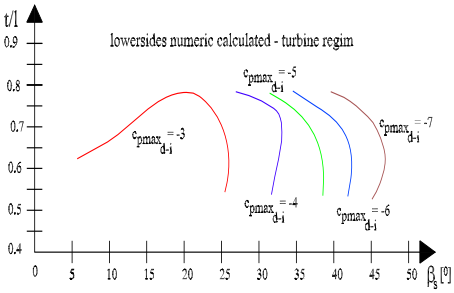

Fig.12 Equal maximum numerical calculated pressure coefficients $c_{p\max}$ = const., on the lower side of the profile DIB-024S from the axial airfoil cascade operating in turbine regime

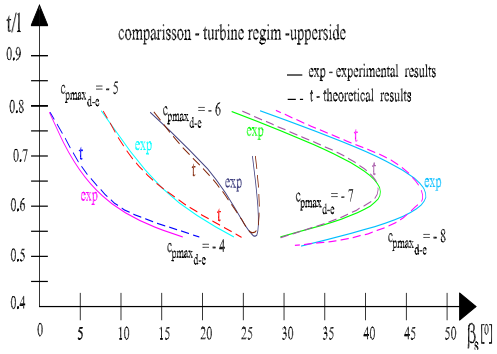

Fig.13 Numeric-experimental comparison of the equal maximum pressure coefficient $c_{p\,max}$ = const., on the upper side of the DIB-024S profile from the axial airfoil cascade in turbine regime

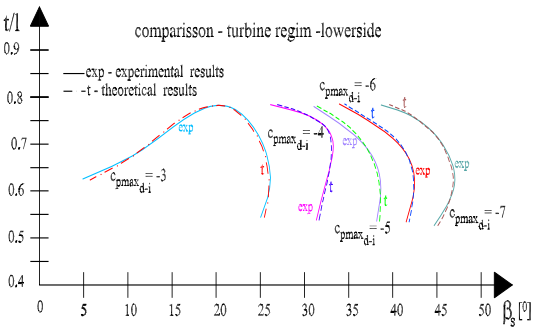

Fig.14 Numeric-experimental comparison of the equal maximum pressure coefficient $c_{p\,max}$ = const., on the lower side of the DIB-024S profile from the axial airfoil cascade in turbine regime

For pump operation regimes these superposition graphics results, for equal maximum pressure coefficient in function of stagger angle β_s and pith to chord ratio t/l, are presented for upper side in fig.15 and for lower side in fig.16, of the DIB-024S type profile from the axial airfoils cascade, in pump regime.

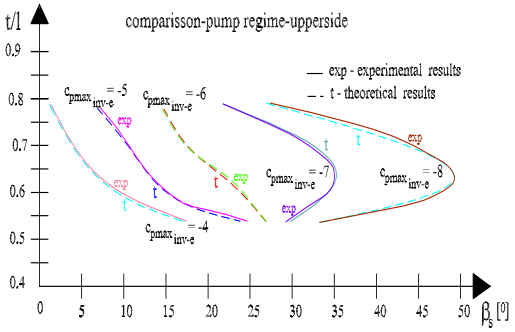

Fig.15 Numeric-experimental comparison of the equal maximum pressure coefficient $c_{p\,max}$ = const., on the upper side of the DIB-024S profile from the axial airfoil cascade in pump regime

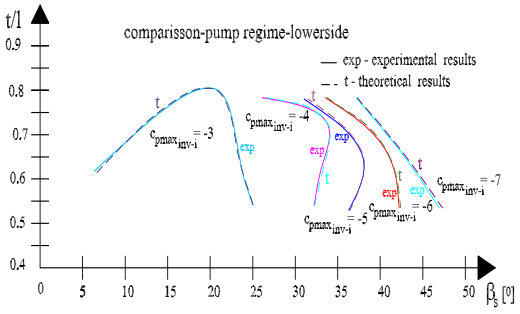

Fig.16 Numeric-experimental comparison of the equal maximum pressure coefficient $c_{p\,max}$ = const., on the lower side of the DIB-024S profile from the axial airfoil cascade in pump regime

Analyzing the theoretical (numerical) and experimental curves, the curves of pitch to chord ratio in function of the stagger angle $t/l = t/l(\beta_s)$ – on which was represented the curves of equal maximum pressure coefficient $c_{p\,max}$ = constant, it is observed the existence of a good agreement and superposition. The calculus with BEM and measurements, on the upper side and lower side of the profile type DIB-024S of the axial airfoils cascades in turbine and pump operation regime and the parameters range of: $t/l = 0.5,\ldots, 0.8$ and $\beta_s = 0,\ldots, 45^0$ gives the same results.

The relative error, between the theoretical curves and the experimental measurements for these distributed parameters don't have values greater than 8%,

and usually values between 4% and 8%. There parts of the curves which overlap each other.

5. Conclusions

1. Boundary Element Method (BEM) for linear elements is an accurate method for solution of fluid flows, in an axial cascade of reversible aerodynamic profiles.
2. Reversible profiles with "S" shape chamber fit very well for pump-turbine blades.
3. The numerical results obtained through BEM on the reversible profile in "S" type DIB-024S, in the axial airfoils cascades was validated through experimental measurements made in the aerodynamic tunnel TLST-40.
4. The good superposition the equal system: pitch to chord ratio-stagger angle, t/l - β_s, is the proof of the precision and efficiency of the BEM.
5. Analyzing the above mentioned curves it is deduced that the small relative error between theory and experiment assures a good quality of the procedure. Maximum values of 8% , usual values between 4% and 8% and zones with superposition are solid arguments for this estimation and assessment.

R E F E R E N C E S

[1] *C.A. Brebbia,* The Boundary Element Method for Engineers, Pentech Press, London, 1978.

[2] *H. Ira Abbot, E. Albert Von Doenhoff,* Theory of Wing Sections, Dover Publications, Inc., **vol. I, II**, New York, 1959.

[3] *I.D. Baciu,* Experimental tests in wind tunnel for an axial cascade of reversible profiles, Hidraulica, Revista de hidraulică –pneumatică – ungere centralizata – mecatronica, nr.1 (18), mai 2006, Editata de Institutul de cercetări pentru hidraulica si pneumatica, ISSN / 1453 – 7303, serie noua, pag. 39-42.

[4] *M. Barglazan, I.D. Baciu,* About Thickness of Aero-Hydrodynamic Profiles, Ştiinţa si inginerie, vol.8, Lucrările celei de a V-a Conferinţe Naţionale multidisciplinare – cu participare internaţională – Profesorul Dorin PAVEL – fondatorul hidroenergeticii româneşti, SEBES, 2005, pag. 79-84, Editura Agir, Bucureşti 2005, ISBN 973-8130-82-4, ISBN 973-720-015-2.

[5] *I.N. Carte, I.D. Baciu,* Velocity and pressure field on the profile boundary of the reversible profile cascades, Fifth International Conference on Hydraulic Machinery and Hydrodynamics., **vol.I** October 2000, pag.23-30, Timişoara, România.

[6] *W. Hackbusch,* Introduction to Multi-grid Methods for the Numerical Solution of Boundary Value Problems, Multigrid Methods Proceeding, p. 46-92, Köln, 1985.

[7] *I. Herrera,* Boundary Methods in Fluids. Finite Elements in Fluids, Volume IV, R.H Gallanger, ed., John Wiley and Sons,1981b

[8] *S. Walker*, Fundamental Solution Progress in Boundary Element Methods, Ed. C.A. Brebbia Pentech Press, 1981.